

Magnetic field effects in the transitions of the HD⁺ molecular ion and precision spectroscopy

D Bakalov¹, V I Korobov² and S Schiller³

¹ Institute for Nuclear Research and Nuclear Energy, Tsarigradsko chaussée 72, Sofia 1784, Bulgaria

² Bogolyubov Laboratory of Theoretical Physics, Joint Institute for Nuclear Research, Dubna 141980, Russia

³ Institut für Experimentalphysik, Heinrich-Heine-Universität Düsseldorf, D-40225 Düsseldorf, Germany

E-mail: dbakalov@inrne.bas.bg

Received 10 October 2010, in final form 20 November 2010

Published 12 January 2011

Online at stacks.iop.org/JPhysB/44/025003

Abstract

We analyse the effects of an external magnetic field on the ro-vibrational, rotational and radiofrequency transitions of the HD⁺ molecular ion—an important systematic effect in precision spectroscopy of HD⁺, which is of interest for metrology of the fundamental constants. The effects of an external magnetic field on the ro-vibrational, rotational and radiofrequency (hyperfine) transitions of the HD⁺ molecular ion are considered, for one-photon and, where relevant, two-photon transitions. The hyperfine structure of the spectrum lines is taken into account. Particular attention has been devoted to those transitions which are most insensitive to the magnetic field and its orientation with respect to the polarization of the radiation field. We identify experimentally accessible two-photon transitions that exhibit no Zeeman shift, one-photon and two-photon transitions that provide symmetrically split doublets, and one-photon transitions that show only a very weak quadratic Zeeman shift. The importance of the spin-stretched states is emphasized. The results can be used to determine the most suitable transitions given the experimental conditions.

1. Introduction

High-precision laser spectroscopy of ultracold hydrogen molecular ions is being considered as a novel approach to (1) measuring and improving the precision of the experimental value of electron-to-proton and proton-to-deuteron mass ratios and (2) strengthening the limits on the time variability of the fundamental constants [1–4]. In order to contribute to improved values and limits, the relative uncertainty of the transition frequency measurements in cases (1) and (2) must be brought down to the 10^{−10} and 10^{−16} levels, respectively. This requires the careful consideration of many systematic effects. One of them is the Zeeman shift due to background or applied magnetic fields.

A small quantization field is typically applied, for example, in order to split the Zeeman components. Undesirable time-dependent magnetic fields may also be present, caused by alternating currents flowing in the ion trap.

Earlier estimates of [5–7] show that the Zeeman shift may significantly exceed the above limits.

The current work presents a complete study of the Zeeman effect in radiofrequency, rotational, and ro-vibrational transitions in HD⁺. As will be shown, both one- and two-photon transitions are of significant potential for precision spectroscopy of HD⁺. Previously, Karr *et al* [8] have evaluated the two-photon transition strengths for HD⁺, but without consideration of hyperfine and Zeeman interactions. Calculations of the Zeeman effect and of the two-photon intensities for the H₂⁺ molecular ion, with account of the hyperfine structure of the states, have been performed in [9, 10]. An analysis of the Zeeman effect on a particular ro-vibrational transition in HD⁺ which was experimentally studied at moderate spectral resolution has been reported in [3].

Having in mind the typical magnetic field strengths in ion traps, we focus our attention on the field range up to 1 G, for which the hyperfine interactions dominate over

the interaction with the external field. The calculations of the spectrum of the lower ro-vibrational states of HD⁺ with total orbital momentum $L \leq 4$ and vibrational quantum number $v \leq 4$ are an extension of the approach developed in previous papers [11–13] for the study of the hyperfine (spin) structure of the transitions. They are needed for the precise comparison with experimental transition frequencies, for selection of appropriate transitions with low sensitivity to external magnetic fields to investigate experimentally, and for evaluation of the experimental uncertainty related to the Zeeman shift in the other cases.

Section 2 describes the evaluation of the energy levels of HD⁺ in constant external magnetic field. We use a Breit-type Hamiltonian to describe the spin interactions in the HD⁺ ion and high-accuracy variational nonrelativistic Coulomb wavefunctions as initial approximation. The relativistic $O(\alpha^2)$ corrections for the magnetic field interaction are neglected since, according to [7], their contribution is small for the magnetic field intensities below 10 G considered here. In sections 3, 4 and 5 we consider the Zeeman effect for the one- and two-photon hyperfine ro-vibrational transition lines, respectively. The main findings are discussed in section 6.

2. Interaction Hamiltonian and hyperfine structure of the energy levels

The spectrum of the HD⁺ ion in an external magnetic field has been calculated using a Hamiltonian that accounts for the electromagnetic interactions of its constituents with each other and with the external magnetic field and has the form $H = H^{\text{NR}} + V^{\text{sh}} + V^{\text{spin}} + V^{\text{mag}}$, where H^{NR} is the non-relativistic 3-body Hamiltonian and the correction terms collect the spin-independent interactions, the spin interactions (cf [12, 13]) and the external magnetic field interaction terms, respectively. The contribution of the spin-independent part of H has been calculated in [14, 15] along with the relativistic and radiative corrections up to order $m\alpha^6$ and including some most important terms of order $m\alpha^7$, and a relative accuracy of 3×10^{-10} has been achieved. It has been shown in [12] that the frequencies of the dominant ‘favoured’ components in the hyperfine multiplet of laser-induced transitions in the absence of external fields can be calculated with a relative accuracy $\sim 5 \times 10^{-10}$ in first order of perturbation theory with a Breit-type spin interaction operator V^{spin} , accurate up to relative order $O(\alpha^2)$. While the work on the derivation of the higher corrections to V^{spin} is currently in progress [16], in the present paper, similar to [12], we restrict ourselves to the leading contributions only; we take the spin interaction Hamiltonian of HD⁺ in an external magnetic field \mathbf{B} to be $V = V^{\text{hfs}} + V^{\text{mag}}$ with V^{mag} in the form

$$V^{\text{mag}} = -\mathbf{m} \cdot \mathbf{B}, \quad \mathbf{m} = \sum_i \frac{eZ_i}{2M_i c} \left(\mathbf{L}_i + \frac{\mu_i}{s_i} \mathbf{S}_i \right), \quad (1)$$

where the summation is over the three constituents of HD⁺ ($i = p, d, e$), Z_i is the electric charge of particle ‘ i ’ in units e , M_i is its mass, μ_i is the magnetic moment in units $e\hbar/2M_i c$, and s_i is the spin (1/2 for $i = p, e$ and 1 for $i = d$).

Table 1. Numerical values of the coefficient E_{10} in the effective spin Hamiltonian of the lower ro-vibrational states of HD⁺, in kHz G⁻¹. E_{10} is zero for $L = 0$.

$L \setminus v$	0	1	2	3	4
1	-0.558 26	-0.553 71	-0.548 86	-0.543 66	-0.538 11
2	-0.558 13	-0.553 56	-0.548 69	-0.543 49	-0.537 92
3	-0.557 92	-0.553 34	-0.548 45	-0.543 22	-0.537 63
4	-0.557 64	-0.553 04	-0.548 13	-0.542 87	-0.537 25

The operators \mathbf{P}_i , \mathbf{R}_i and $\mathbf{L}_i = \mathbf{R}_i \times \mathbf{P}_i$ are respectively the momenta, position vectors and orbital momenta of the particles in the centre-of-mass frame, \mathbf{S}_i are the spin operators, and \mathbf{B} is the external magnetic field. We neglect the effects of the non-separability of the centre-of-mass motion that is justified for magnetic field intensities of a few Gauss [17].

Compared to the Hamiltonian of [7], V^{mag} contains only the leading-order terms; the relativistic corrections to V^{mag} of relative order $O(\alpha^2)$ have been omitted. This is a reasonable approximation for magnetic fields B for which the contribution of V^{mag} does not exceed the contribution of V^{spin} . For this case the contribution of the relativistic corrections to V^{mag} is smaller than the uncertainty of the theoretical results on the hyperfine energy levels of [12].

We calculate the spin structure of a ro-vibrational state (v, L) in first order of perturbation using the state-dependent ‘effective spin Hamiltonian’ $H_{\text{eff}}^{\text{tot}}$ obtained by averaging $V^{\text{spin}} + V^{\text{mag}}$ over the spatial degrees of freedom:

$$H_{\text{eff}}^{\text{tot}} = H_{\text{eff}}^{\text{hfs}} + E_{10}(\mathbf{L} \cdot \mathbf{B}) + E_{11}(\mathbf{S}_p \cdot \mathbf{B}) + E_{12}(\mathbf{S}_d \cdot \mathbf{B}) + E_{13}(\mathbf{S}_e \cdot \mathbf{B}), \quad (2)$$

where $H_{\text{eff}}^{\text{hfs}}$ is the effective Hamiltonian of HD⁺ in the absence of magnetic field given in (3) of [12]. The coefficients E_{11} , E_{12} , and E_{13} in the adopted approximation are obtained directly from (1) and are expressed in terms of masses and magnetic moments of particles,

$$E_{11} = -\frac{e\mu_p}{M_p c} = -4.2577 \text{ kHz G}^{-1},$$

$$E_{12} = -\frac{e\mu_d}{2M_d c} = -0.6536 \text{ kHz G}^{-1},$$

$$E_{13} = \frac{e\mu_e}{M_e c} = 2.8025 \text{ MHz G}^{-1}.$$

The value of E_{10} is calculated using the variational nonrelativistic wavefunctions of HD⁺ of [14]:

$$E_{10} = -\mu_B \sum_i \frac{Z_i M_e}{M_i} \frac{\langle vL || \mathbf{L}_i || vL \rangle}{\sqrt{L(L+1)(2L+1)}}.$$

The results are given in table 1. Hegstrom [7] calculated E_{10} obtaining a value $-0.528 \text{ kHz G}^{-1}$ with estimated ro-vibrational level-dependent corrections on the order of a few per cent for the low-lying levels, which is consistent with the values in table 1.

The spin splitting of the energy levels of HD⁺ is evaluated by diagonalizing the matrix of $H_{\text{eff}}^{\text{tot}}$. The coupling scheme is the same as in [12]:

$$\mathbf{F} = \mathbf{S}_p + \mathbf{S}_e, \quad \mathbf{S} = \mathbf{F} + \mathbf{S}_d, \quad \mathbf{J} = \mathbf{S} + \mathbf{L}. \quad (3)$$

An appropriate basis set \mathcal{F} are the vectors with definite values of the squared angular momenta \mathbf{F}^2 , \mathbf{S}^2 , \mathbf{J}^2 and z -axis

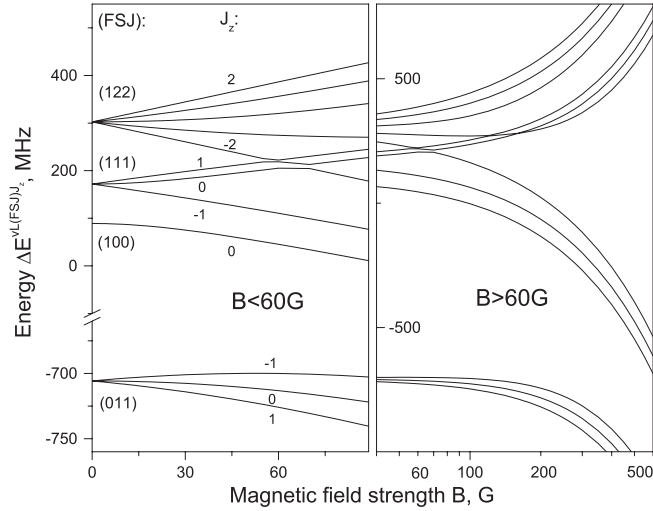


Figure 1. Energies $\Delta E^{vL(FSJ)J_z}$ of the hyperfine levels of the ground ro-vibrational state ($v = 0, L = 0$) of HD^+ versus the magnetic field B at low ($B < 60$ G, left) and high ($B > 60$ G, right) magnetic field strength. The two stretched states are the top and bottom sub-levels of the level at ~ 300 MHz.

projection J_z of \mathbf{J} . $|LFSJJ_z\rangle$. Of these, J_z is the only exact quantum number for the nonzero field B with the exception of the ‘stretched’ states with $F = S_p + S_e = 1, S = F + S_d = 2, J = S + L = L + 2$ and $J_z = \pm J$, for which $F, S,$ and J are also exact quantum numbers. Labelling the eigenstates of $H_{\text{eff}}^{\text{tot}}$ therefore requires an additional index n . The eigenvalues of $H_{\text{eff}}^{\text{tot}}, \Delta E^{vLnJ_z}$, represent the energy levels of HD^+ , defined relative to the ‘spinless’ energies E^{vL} (i.e. the eigenvalues of H^{NR} , corrected with the contribution of V^{diag}). ΔE^{vLnJ_z} and the coefficients $\beta_{FSJ}^{vLnJ_z}$ of the corresponding state vectors in the basis \mathcal{F} ,

$$|vLnJ_z\rangle = \sum_{FSJ} \beta_{FSJ}^{vLnJ_z} |LFSJJ_z\rangle,$$

are calculated from the system of equations

$$\begin{aligned} \sum_{F'S'J'} \langle LFSJJ_z | H_{\text{eff}}^{\text{tot}} | L'F'S'J' J_z \rangle \beta_{F'S'J'}^{vLnJ_z} \\ = \Delta E^{vLnJ_z} \beta_{FSJ}^{vLnJ_z}. \end{aligned} \quad (4)$$

We take for n the set of quantum numbers $n = (F, S, J)$ used to label the hyperfine states in the absence of magnetic fields; F, S and J are ascribed the values of the corresponding quantum numbers of the basis vector $|LFSJJ_z\rangle$ for which $|\beta_{FSJ}^{vLnJ_z}|$ is maximal. This is applicable for the magnetic fields B that are sufficiently low so that no avoided crossings of levels with the same J_z take place. As an example, figure 1 shows the hyperfine energies $\Delta E^{vLnJ_z}(B)$ of the ground state $(v, L) = (0, 0)$ of HD^+ as a function of the magnetic field B ; no avoided crossings occur in this particular case. The level diagrams of the lower rotationally excited states look similar, except for the much larger number of sub-levels; the first avoided crossings typically take place at $B \sim 20\text{--}40$ G, but may occur even at $B = 2$ G, as is the case with the $(v = 2, L = 4)$ state.

In the presence of a magnetic field, the hyperfine states of HD^+ labelled with F, S and J (cf [12]) are split into sub-levels

distinguished by means of the quantum number J_z . At low magnetic fields the dependence of $\Delta E^{vLnJ_z}(B)$ on B may be approximated with the quadratic form

$$\begin{aligned} (\Delta E^{vLnJ_z}(B) - \Delta E^{vLnJ_z}(0))/h \\ \approx t^{vLn} \cdot J_z \cdot B + (q^{vLn} + r^{vLn} \cdot J_z^2) \cdot B^2, \end{aligned} \quad (5)$$

which reproduces the exact values with a relative error below 10^{-6} for $B < 1$ G except for the Zeeman components of the $L = 1$ states with $F = 1, S = 2, J = 2, 3$ and very close hyperfine energies, for which the contribution of third order in B cannot be neglected and relative accuracy better than 10^{-5} cannot be achieved without a higher order polynomial fit. Relation (5) will be used to evaluate the shift of laser or radiofrequency-driven transition frequencies to external magnetic fields and choose the less sensitive ones as candidates for precision spectroscopy. The values of t^{vLn}, q^{vLn} and r^{vLn} for the lower ro-vibrational states with $v \leq 4$ and $L \leq 4$ are given in table 2. The term quadratic in B is of interest mainly for the states with $J_z = 0$, and gives an observable contribution for the remaining states at $B > 0.1$ G. The rearrangement of the spectrum starts above 50 G; at high B the spectrum acquires doublet form due to the domination of the term $E_{13}(\mathbf{S}_e \cdot \mathbf{B})$ in $H_{\text{eff}}^{\text{tot}}$, while the small splitting of each branch is due to the $E_{11}(\mathbf{S}_p \cdot \mathbf{B})$ term whose contribution is next in size.

2.1. Stretched states

The energies of the two stretched states in an external magnetic field can be given in a simple analytical form:

$$\begin{aligned} \Delta E^{vL(1,2,L+2)\pm(L+2)}(B)/h \\ = \pm(2 E_{10}L + E_{11} + 2 E_{12} + E_{13})B/2 + E_4/4 + E_5/2 \\ + (E_1 + E_2 + 2E_3 + E_6 + 2E_7 + 2E_8 + E_9)L/2 \\ - (2E_6 + 4E_7 + 4E_8 + 2E_9)L^2/2. \end{aligned} \quad (6)$$

Thus, the magnetic shift is *strictly* linear in B ($q^{vLn} + r^{vLn}(L+2)^2 = 0$), with

$$t^{vLn} = (LE_{10} + E_{12} + (E_{11} + E_{13})/2)/(L+2).$$

The numerical values of t^{vLn} for the stretched states can be found in the column labelled $J = L + 2$ of table 2. While the numerical values of q^{vLn} and r^{vLn} therein do not exactly satisfy the above relation, the contribution of the quadratic term on B does not exceed the relative error limit of 10^{-6} except for the stretched states with $L = 1$, as already discussed. The selection rules for electric dipole (E1) transitions read $L' - L = \pm 1, |J'_z - J_z| \leq 1$ for one-photon transitions and $L' - L = 0, \pm 2, J'_z - J_z = 0, \pm 2$ for two-photon transitions (see below for restrictions); therefore, transitions between stretched states are possible and deserve special attention. We immediately recognize that the transitions between a lower stretched state $vL(1, 2, L+2)J_z$ and an upper stretched state $v'L'(1, 2, L'+2)J'_z$ with either $J_z = L+2 \rightarrow J'_z = L'+2$ or $J_z = -(L+2) \rightarrow J'_z = -(L'+2)$ form a doublet except for the special case $L = L' = 0$. Due to the independence of E_{11}, E_{12}, E_{13} on the ro-vibrational state, the respective shifts, $\pm(E_{10}(v', L')L' - E_{10}(v, L)L)$, have the same magnitude and opposite signs. We can distinguish the cases.

- (i) One-photon transitions: the splitting is of order $\pm 0.5 \text{ kHz G}^{-1}$.
- (ii) Two-photon transitions with $L' - L = \pm 2$: the splitting is of order $\pm 1 \text{ kHz G}^{-1}$.
- (iii) Two-photon transitions with $L' = L \neq 0$: the splitting is of order $\pm 10 \text{ Hz G}^{-1}$, since E_{10} varies weakly with the vibrational quantum number.
- (iv) Two-photon transitions with $L' = L = 0$: no splitting.

In all cases, the mean frequency of the doublet is *independent* of the magnetic field.

3. Zeeman structure of the one-photon $E1$ transition spectrum

The probability per unit time $P_{fi}^{(1)}(\nu)$ for electric dipole transition between an initial (lower) $|i\rangle \equiv |vLnJ_z\rangle$ and final (upper) $\langle f| \equiv \langle v'L'n'J'_z|$ state, stimulated by an oscillating linearly polarized electric field $\mathbf{E}(t) = \mathbf{E} \cos 2\pi\nu t$ of frequency ν , is

$$P_{fi}^{(1)}(\nu) = (1/4\hbar^2)\delta(\nu - \nu_{fi})|\langle f|W|i\rangle|^2, \quad (7)$$

where

$$\nu_{fi} = \nu_0 + (\Delta E^{v'L'n'J'_z} - \Delta E^{vLnJ_z})/h,$$

and $\nu_0 = (E^{v'L'} - E^{vL})/h$ is referred to as ‘central frequency’, $W = -\mathbf{E} \cdot \mathbf{d}$ is the interaction with the electric field, and $\mathbf{d} = \sum_i Z_i \mathbf{R}_i$ is the electric dipole moment operator. Linear polarization will be assumed in what follows as well. We have

$$\langle f|W|i\rangle = \sum_{q=0,\pm 1} E^q A_q^{fi} \quad (8)$$

with

$$\begin{aligned} A_q^{fi} &= \langle v'L'n'J'_z|\mathbf{d}_q|vLnJ_z\rangle \\ &= d_{fi} \sum_{J'JFS} \sqrt{2J+1} C_{JJ_z,1q}^{J'J'_z} \begin{Bmatrix} J' & 1 & J \\ L & S & L' \end{Bmatrix} \\ &\times (-)^{J'+L+S} \beta_{FSJ'}^{v'L'n'J'_z} \beta_{FSJ}^{vLnJ_z}, \end{aligned} \quad (9)$$

where d_{fi} are the reduced matrix elements of \mathbf{d} which, in the non-relativistic approximation, do not depend on the spin quantum numbers: $d_{fi} \equiv d_{v'L',vL}$. $C_{\alpha\alpha,\beta\beta}^{c\gamma}$ are Clebsch–Gordan coefficients, and E^q denote the cyclic components of \mathbf{E} that are expressed in terms of the amplitude $|\mathbf{E}|$ of the oscillating electric field and the angle θ between \mathbf{E} and the external magnetic field \mathbf{B} : $E^{\pm 1} = \mp |\mathbf{E}| \sin\theta/\sqrt{2}$, $E^0 = |\mathbf{E}| \cos\theta$. The numerical values of $d_{v'L',vL}$ for the transitions of interest, calculated with the variational Coulomb wavefunctions of [14], are given in table 3 and agree with the results of [18] at the 10^{-3} level.

The observable $E1$ transition spectrum

$$I(\nu) = \sum_{f,i} w_i P_{fi}^{(1)}(\nu) \quad (10)$$

can then be put in the form

$$I(\nu) = |\mathbf{E}|^2 \sum_{f,i} \frac{w_i}{4\hbar^2} \delta(\nu - \nu_{fi}) T_{fi}^{(1)}(\theta), \quad (11)$$

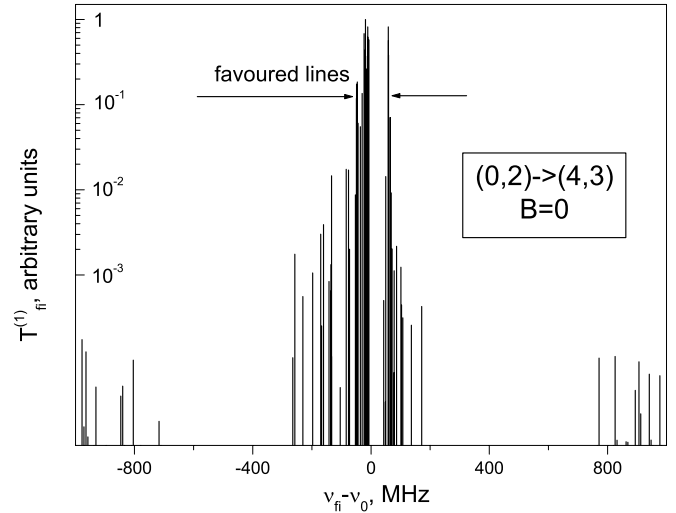


Figure 2. Left: strength $T_{fi}^{(1)}$ of the hyperfine components of the $(v, L) = (0, 2) \rightarrow (4, 3)$ one-photon $E1$ transition line at $B = 0$ (no θ -dependence). While the entire spectrum spreads over a GHz range, the dominating favoured components lie in a bandwidth of ~ 100 MHz around the central frequency ν_0 .

with

$$T_{fi}^{(1)}(\theta) = \cos^2\theta (A_0^{fi})^2 + \frac{\sin^2\theta}{2} [(A_{-1}^{fi})^2 + (A_1^{fi})^2].$$

The sum is over all pairs of states (i, f) belonging to the hyperfine structure of the initial and final ro-vibrational states that are coupled by W , and w_i is the population of the initial state. The number of sub-lines (summands in (11)) may exceed 10^3 , but most of them are weak as shown in figure 2. For magnetic fields B below 50 G the spectrum $I(\nu)$ is dominated by the ‘favoured’ transitions between states with homologous spin structure that, in addition to the general selection rule $|\Delta J| \leq 1$, also satisfy $\Delta S = \Delta F = 0$; the frequencies of the favoured transitions lie in a bandwidth of ~ 100 MHz around ν_0 . The other hyperfine lines have intensities smaller by orders of magnitude and would be difficult to observe in an experiment.

Recently, a measurement of the spectrum of the $(0, 2) \rightarrow (4, 3)$ transition with 2-ppb accuracy has been performed in magnetic fields B not exceeding 1 G [3]. The spectroscopic resolution of ~ 50 MHz did not allow for distinguishing the individual hyperfine lines or their Zeeman subcomponents. When the spectroscopic resolution is this low, one can consider the weighted mean of the Zeeman shifts over all lines as an estimate of the systematic contribution due to the Zeeman effect. Considering the lines in the range from -75 to 75 MHz of the mentioned ro-vibrational transition yields less than 1 kHz shift at $B = 1$ G, a very small value compared to the assumed spectroscopic resolution.

The next level of experimental resolution is when the individual hyperfine lines can be resolved, but not the Zeeman subcomponents. Compared with the situation in the absence of external fields, the observable transition lines are *broadened* and *shifted*. To estimate the shift, we consider the weighted

Table 3. Reduced matrix elements $d_{v'L',vL} = \langle v'L' || \mathbf{d} || vL \rangle$ of the electric dipole moment of HD⁺, in Debye. The notation $a(b)$ stands for $a \times 10^b$.

v'	v	$d_{v'1,v0}$	$d_{v'2,v1}$	$d_{v'3,v2}$	$d_{v'4,v3}$	$d_{v'5,v4}$
0	0	0.87140(+0)	0.12341(+1)	-0.15151(+1)	-0.17553(+1)	-0.19709(+1)
0	1	-0.94562(-1)	-0.13970(+0)	-0.17847(+0)	0.21466(+0)	0.24966(+0)
0	2	-0.11336(-1)	-0.16164(-1)	0.19925(-1)	-0.23119(-1)	0.25934(-1)
0	3	-0.24679(-2)	0.34659(-2)	0.42077(-2)	0.48085(-2)	-0.53128(-2)
0	4	-0.72966(-3)	0.10156(-2)	0.12216(-2)	0.13834(-2)	0.15147(-2)
1	0	-0.86264(-1)	0.11624(+0)	0.13543(+0)	0.14850(+0)	-0.15738(+0)
1	1	0.92088(+0)	-0.13041(+1)	0.16008(+1)	-0.18542(+1)	0.20814(+1)
1	2	-0.13526(+0)	0.20006(+0)	0.25586(+0)	-0.30807(+0)	-0.35865(+0)
1	3	-0.19660(-1)	-0.28068(-1)	0.34641(-1)	0.40242(-1)	0.45196(-1)
1	4	-0.48795(-2)	-0.68626(-2)	0.83441(-2)	0.95494(-2)	-0.10565(-1)
2	0	-0.11091(-1)	-0.15469(-1)	-0.18647(-1)	0.21151(-1)	0.23183(-1)
2	1	-0.12307(+0)	-0.16560(+0)	0.19264(+0)	0.21089(+0)	0.22311(+0)
2	2	0.97207(+0)	0.13765(+1)	0.16894(+1)	0.19565(+1)	-0.21957(+1)
2	3	-0.16764(+0)	0.24824(+0)	-0.31785(+0)	0.38311(+0)	-0.44645(+0)
2	4	-0.27889(-1)	0.39866(-1)	-0.49262(-1)	0.57300(-1)	0.64435(-1)
3	0	0.24882(-2)	-0.35228(-2)	0.43101(-2)	-0.49613(-2)	0.55177(-2)
3	1	0.19185(-1)	-0.26723(-1)	-0.32172(-1)	-0.36445(-1)	0.39893(-1)
3	2	0.15213(+0)	-0.20440(+0)	0.23740(+0)	0.25946(+0)	0.27400(+0)
3	3	-0.10252(+1)	-0.14516(+1)	-0.17814(+1)	0.20627(+1)	0.23143(+1)
3	4	0.19599(+0)	0.29059(+0)	0.37249(+0)	-0.44946(+0)	0.52430(+0)
4	0	0.74954(-3)	-0.10707(-2)	0.13218(-2)	0.15349(-2)	0.17217(-2)
4	1	0.49098(-2)	-0.69438(-2)	-0.84853(-2)	0.97555(-2)	0.10837(-1)
4	2	0.27142(-1)	-0.37759(-1)	0.45401(-1)	-0.51361(-1)	0.56142(-1)
4	3	0.17737(+0)	0.23796(+0)	0.27593(+0)	0.30104(+0)	-0.31731(+0)
4	4	-0.10805(+1)	-0.15298(+1)	-0.18772(+1)	-0.21733(+1)	-0.24380(+1)

Table 4. Offset of the hyperfine transition frequencies $\bar{\nu} \equiv \bar{\nu}_{v'L'n'J'_z,vLnJ_z}(0)$ in the absence of magnetic field with respect to the central frequency ν_0 (in MHz), and shift $\delta\bar{\nu} \equiv \delta\bar{\nu}_{v'L'n',vLn}(B) = \bar{\nu}_{v'L'n',vLn}(B) - \bar{\nu}_{v'L'n',vLn}(0)$ of the weighted mean frequencies of the multiplets of magnetic components of six favoured hyperfine lines ($FSJ \rightarrow FSJ'$), $J' = J + 1$, in the $E1$ transition ($vL) = (0, 2) \rightarrow (4, 3)$, calculated for the external magnetic field $B=0.5$ G and 1 G, parallel ($\theta = 0$) or orthogonal ($\theta = \pi/2$) to the oscillating electric field (in kHz).

(F, S, J)	(1, 2, 3)		(1, 2, 1)		(1, 1, 2)		(0, 1, 3)		(0, 1, 2)		(0, 1, 1)	
$\bar{\nu} - \nu_0$, MHz	-23.481		-14.257		-6.902		58.251		58.861		59.426	
$\theta =$	0	$\pi/2$	0	$\pi/2$	0	$\pi/2$	0	$\pi/2$	0	$\pi/2$	0	$\pi/2$
$\delta\bar{\nu}(0.5 \text{ G})$, kHz	5.1	5.1	-1.5	-3.0	-1.4	-2.7	-0.1	0.1	-0.2	-0.1	0.0	-0.1
$\delta\bar{\nu}(1.0 \text{ G})$, kHz	16.9	17.0	-5.1	-9.8	-4.8	-8.7	-0.3	0.4	-0.5	-0.1	0.0	-0.5

mean frequency $\bar{\nu}_{v'L'n',vLn}(B)$ of the multiplet of magnetic components of the hyperfine transition ($vLn) \rightarrow (v'L'n')$:

$$\bar{\nu}_{v'L'n',vLn}(B) = \frac{\sum_{J'_z, J_z} \nu_{fi} | \langle f | W | i \rangle |^2}{\sum_{J'_z, J_z} | \langle f | W | i \rangle |^2}, \quad (12)$$

where the summation is restricted to the Zeeman subcomponents of the multiplet and uniform population of the J_z Zeeman sub-levels is assumed. The shift of $\bar{\nu}_{v'L'n',vLn}$ depends nonlinearly on B and at $B \sim 0.5$ G may already exceed the near-future target uncertainty for QED tests and measurement of particle masses. Table 4 gives the values of the weighted mean frequencies $\bar{\nu}_{v'L'n',vLn}(B)$ at $B = 0$ and their Zeeman shifts, $\delta\bar{\nu}_{v'L'n',vLn}(B) = \bar{\nu}_{v'L'n',vLn}(B) - \bar{\nu}_{v'L'n',vLn}(0)$, for six favoured hyperfine lines in the spectral range investigated in [3], for magnetic fields $B = 0.5$ and 1 G, either parallel or orthogonal to the electric field polarization. The first three lines in the list are rather well separated, by a few MHz, from adjacent favoured ones (not listed). $\bar{\nu}_{v'L'n',vLn}(B)$ cannot be correctly calculated for the pairs of lines whose hyperfine multiplets overlap. The shift of $\bar{\nu}_{v'L'n',vLn}$ for some

lines may reach many kHz for B of the order of 1 G, while other lines have substantially less magnetic field sensitivity.

Future spectroscopic measurements of HD⁺ are expected to reach a resolution that will make it possible to separate the individual Zeeman components. At low B the magnetic shift of the resonance frequency of a single Zeeman component may be estimated using the approximation of (5):

$$\delta\nu_{fi}(B) = \nu_{v'L'n'J'_z,vLnJ_z}(B) - \nu_{v'L'n'J'_z,vLnJ_z}(0) \approx (t'J'_z - tJ_z)B + (q' - q)B^2, \quad (13)$$

where t' , q' and t , q refer to the final and initial states, respectively. The systematic uncertainty related to the external magnetic field will be minimized by selecting transitions with minimal $\delta\nu_{fi}(B)$; the latter can be achieved for transitions with $J'_z = J_z = 0$ (thus eliminating the large linear dependence on B), with close numerical values of q' and q that cancel each other. A few examples of such transitions with very low magnetic field sensitivity and sufficient strength are listed in table 5. For the pure rotational transition (first line) the shift relative to the transition frequency is 3×10^{-12} , while for the

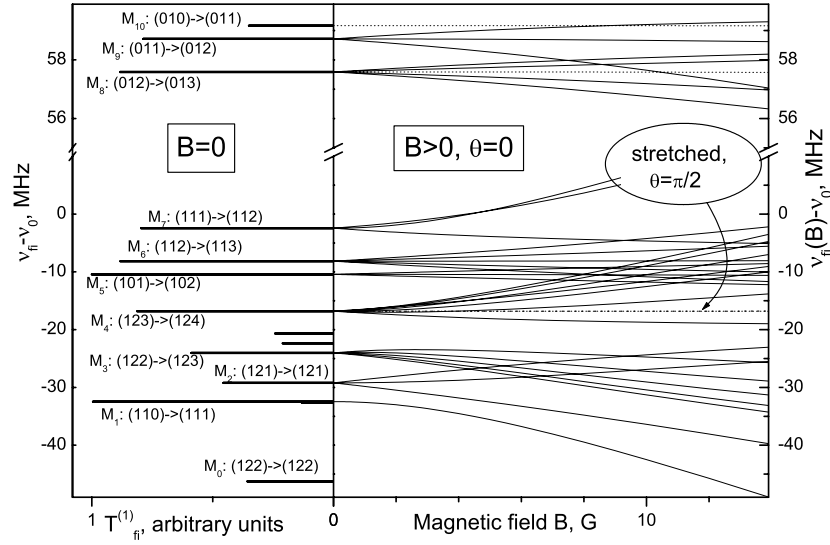


Figure 3. Left: strength $T_{fi}^{(1)}$ of ten favoured hyperfine components M_0, \dots, M_{10} of the $(v, L) = (0, 1) \rightarrow (4, 2)$ one-photon $E1$ transition line at $B = 0$ (no θ -dependence), labelled with the quantum numbers (FSJ) of the initial and final states. Right: frequencies of the $\Delta J_z = 0$ components of M_1, \dots, M_{10} as a function of the magnetic field B for $\theta = 0$. The $J_z = 0 \rightarrow J_z = 0$ components of M_8 and M_{10} (short dotted lines) undergo a very small quadratic shift. The frequencies of the transitions between stretched states in the transversal field (dotted lines) have a very small linear shift; their mean is independent of B .

Table 5. Examples of favoured one-photon $E1$ transitions $(vL(FSJ)J_z = 0) \rightarrow (v'L'(F'S'J')J'_z = 0)$ with zero linear magnetic shift and low quadratic magnetic field sensitivity $q' - q = \delta v_{fi}(B)/B^2$.

v	L	F	S	J	J_z	\rightarrow	v'	L'	F'	S'	J'	J'_z	$q' - q, \text{Hz G}^{-2}$
0	1	0	1	1	0		0	2	0	1	2	0	8
0	1	1	1	2	0		3	2	1	1	3	0	22
0	1	0	1	0	0		4	2	0	1	1	0	-16
0	1	0	1	2	0		4	2	0	1	3	0	-38
0	2	0	1	2	0		4	3	0	1	3	0	-37

vibrational transitions the lowest relative shift is -7×10^{-14} (third line).

There also exist transitions between the states of nonzero magnetic quantum number J_z and J'_z with suppressed magnetic field sensitivity, e.g. $|vL(FSJ)J_z\rangle = |02(011)-1\rangle \rightarrow |43(012)-2\rangle$ for which $|\delta v_{fi}(B)| < 81 \text{ Hz}$ for $B \leq 0.5 \text{ G}$.

Of particular interest are the transitions between stretched states: the strictly linear magnetic shift of the transition frequencies is $\pm(L'E'_{10} - LE_{10})B$ with L, E_{10} (L', E'_{10}) referring to the initial (final) state. In the case of a one-photon transition, the selection rule is $L - L' = \pm 1$, and the shift amounts to about $\pm 0.5 \text{ kHz}$ for $B = 1 \text{ G}$. The mean frequency of the pair of transitions is independent of B .

One candidate for one-photon spectroscopy of HD^+ is the $\lambda \approx 1.4 \mu\text{m}$ transition $(v, L) = (0, 1) \rightarrow (4, 2)$. The hyperfine spectrum includes 18 favoured lines, of which 10 (M_1, \dots, M_{10}) are shown in figure 3, left. While most of them are quite sensitive to the external magnetic field strength (figure 3, right), the frequencies of the $J'_z = J_z = 0$ components of M_8 and M_{10} transitions for longitudinal magnetic field ($\theta = 0$) have a very weak quadratic Zeeman shift. The third transition in table 4 (approx. 59.2 MHz) belongs to M_{10} , while the fourth transition in table 4 (approx. 57.6 MHz) belongs to the M_8 line. Line M_4 (approx.

-16.8 MHz) contains the stretched state transitions, but these are not shown in figure 3 (right), since they only occur for perpendicular polarization, $\theta = \pi/2$.

4. One-photon magnetic $M1$ transitions

In addition to the one-photon $E1$ -transitions discussed above, of interest are the $M1$ -transitions between states of the hyperfine structure of a single (vL) state, stimulated by an oscillating magnetic field $\mathbf{B}'(t) = \mathbf{B}' \cos 2\pi\nu t$ of frequency ν in the microwave region. Similar to (11), the observable microwave spectrum $I'(\nu)$ is

$$I'(\nu) = |\mathbf{B}'|^2 \sum_{fi} \frac{w_i}{4\hbar^2} \delta(\nu - \nu_{fi}) T_{fi}^{(1)}(\theta), \quad (14)$$

$$T_{fi}^{(1)}(\theta) = \cos^2 \theta' (A_0^{'fi})^2 + \frac{\sin^2 \theta'}{2} [(A_{-1}^{'fi})^2 + (A_1^{'fi})^2]$$

where $A_q^{'fi} = \langle vLn'J'J'_z | \mathbf{m}_q | vLnJJ_z \rangle$, \mathbf{m} is the magnetic dipole moment of HD^+ defined in (1), and θ' is the angle between the oscillating (\mathbf{B}') and the external magnetic field (\mathbf{B}). The explicit expression of the matrix elements of \mathbf{m} between states with the same values of v and L reads

$$A_q^{'fi} = E_{11} A_q^{(p)fi} + E_{12} A_q^{(d)fi} + E_{13} A_q^{(e)fi} + E_{10} A_q^{(L)fi},$$

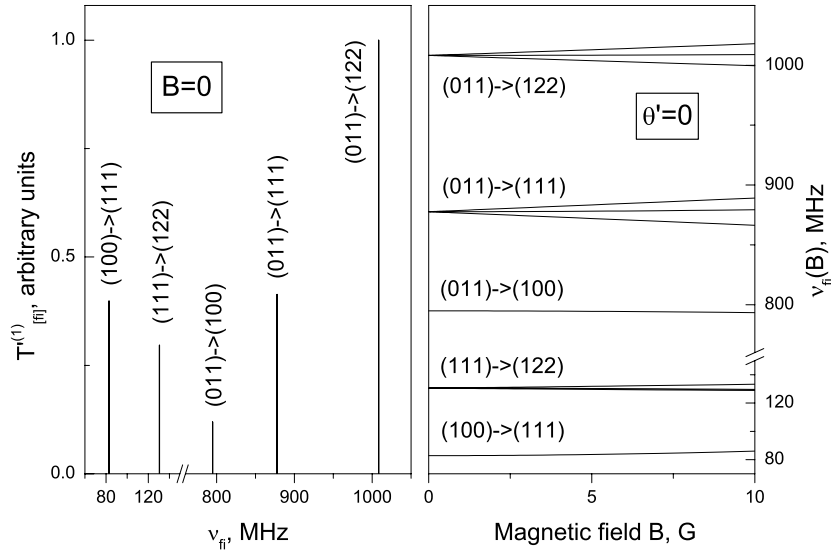


Figure 4. Strength $T_{fi}^{(1)}(\theta')$ of the $M1$ -transitions between the hyperfine states of the ground state $(0, 0)$ of HD^+ in the absence of external magnetic field ($B = 0$, no θ' -dependence), and transition frequencies $\nu_{fi}(B)$ for $B < 10$ G stimulated by an oscillating magnetic field \mathbf{B}' parallel to the external field \mathbf{B} .

$$\begin{aligned}
A_q^{(d)fi} &= (-1)^{J+L-F-1} \delta_{F'F} \sqrt{6} \Pi_{JF'F} \\
&\times \begin{Bmatrix} S & 1 & S' \\ J' & L & J \end{Bmatrix} \begin{Bmatrix} 1 & 1 & 1 \\ S' & F & S \end{Bmatrix} C_{JJ_z, 1q}^{J'J_z}, \\
A_q^{(p)fi} &= (-1)^{J+L+F'+F+S'+S-1} \sqrt{\frac{3}{2}} \Pi_{JS'S'F'S} \\
&\times \begin{Bmatrix} S & 1 & S' \\ J' & L & J \end{Bmatrix} \begin{Bmatrix} F & 1 & F' \\ S' & 1 & S \end{Bmatrix} \begin{Bmatrix} 1/2 & 1 & 1/2 \\ F' & 1/2 & F \end{Bmatrix} C_{JJ_z, 1q}^{J'J_z}, \\
A_q^{(e)fi} &= (-1)^{F'+F} A_q^{(p)fi}, \\
A_q^{(L)fi} &= \delta_{F'F} \delta_{S'S} (-1)^{J+L+S-1} \Pi_J \\
&\times \begin{Bmatrix} L & 1 & L \\ J' & S & J \end{Bmatrix} \sqrt{L(L+1)(2L+1)} C_{JJ_z, 1q}^{J'J_z}, \quad (15)
\end{aligned}$$

where the notation $\Pi_{ab\dots} = \sqrt{(2a+1)(2b+1)\dots}$ is used. Equation (15) shows that radiofrequency transitions are mainly due to the $(\mathbf{B}' \cdot \mathbf{S}_e)$ term in V^{mag} . The frequencies ν_{fi} of the transitions with $\Delta F = \pm 1$ are typically in the range $700 < \nu_{fi} < 1100$ MHz, while, for $\Delta F = 0$, $\nu_{fi} < 200$ MHz. Figure 4 presents the microwave spectrum of the ground state $(0, 0)$ of HD^+ for external magnetic fields below 10 G.

5. Hyperfine structure of the laser-excited two-photon transition spectrum

Two-photon spectroscopy [19, 22] of ultra-cold HD^+ ions is of interest since it can be implemented with counter-propagating beams and is therefore free of first-order Doppler broadening. Accounting for the effects of external magnetic field becomes particularly important in this case.

Using the notations of section 3, we put the probability per unit time $P_{fi}^{(2)}(\nu)$ for a two-photon transition of HD^+ in the form

$$\begin{aligned}
P_{fi}^{(2)}(\nu) &= \frac{1}{32} \delta\left(\nu - \frac{\nu_{fi}}{2}\right) \left| \sum_{q',q} E^{q'} E^q A_{q'q}^{(2)fi} \right|^2 \\
&= \frac{1}{32} \delta\left(\nu - \frac{\nu_{fi}}{2}\right) |\mathbf{E}|^4 T_{fi}^{(2)}(\theta); \quad (16)
\end{aligned}$$

$$\begin{aligned}
T_{fi}^{(2)}(\theta) &= \frac{1}{4} \sin^4 \theta [(A_{-1-1}^{(2)fi})^2 + (A_{11}^{(2)fi})^2] \\
&+ \frac{1}{2} \sin^2 \theta \cos^2 \theta [(A_{-10}^{(2)fi} + A_{0-1}^{(2)fi})^2 + (A_{01}^{(2)fi} + A_{10}^{(2)fi})^2] \\
&+ \frac{1}{4} [\sin^2 \theta (A_{-11}^{(2)fi} + A_{1-1}^{(2)fi}) - 2 \cos^2 \theta A_{00}^{(2)fi}]^2 \quad (17)
\end{aligned}$$

where $A_{q'q}^{(2)fi} = \sum_k A_{q'k}^{fk} (\nu - \nu_{ki})^{-1} A_q^{ki}$ and k stands for the quantum numbers $(\nu_k, L_k, n_k = (F_k, S_k, J_k), J_{kz})$ of the intermediate states of HD^+ . The sum over k is restricted to states for which $L_k = L \pm 1$, $L' = L_k \pm 1$, $J_{kz} = J_z + q$ and $J'_z = J_{kz} + q'$.

Some general transition rules should be noted [19]:

- (i) for transitions with $\Delta L = 2$, $J = 0 \rightarrow J' = 0$ is forbidden, $J = 0 \rightarrow J' = 1$ is forbidden, and for $J, J_z \rightarrow J' = J + 1$, J'_z the case $J_z = J'_z$ is forbidden;
- (ii) for transitions with $\Delta L = 0$, and $L = 0 \rightarrow L' = 0$, only $J, J_z \rightarrow J' = J$, $J'_z = J_z$ are allowed;
- (iii) for transitions with $\Delta L = 0$, and $L \neq 0 \rightarrow L' = L$, the case $J = 0, J_z \rightarrow J' = 1, J'_z = J_z$ is forbidden;
- (iv) for transitions with $\Delta L = 0$, and $J_z \neq J'_z$, the cases $J = 0 \rightarrow J' = 0$ and $J = 0 \rightarrow J' = 1$ are forbidden.

General features of two-photon transition spectra of HD^+ are illustrated in the example of the $(0, 2) \rightarrow (4, 2)$ transition. Favoured hyperfine components in the absence of magnetic

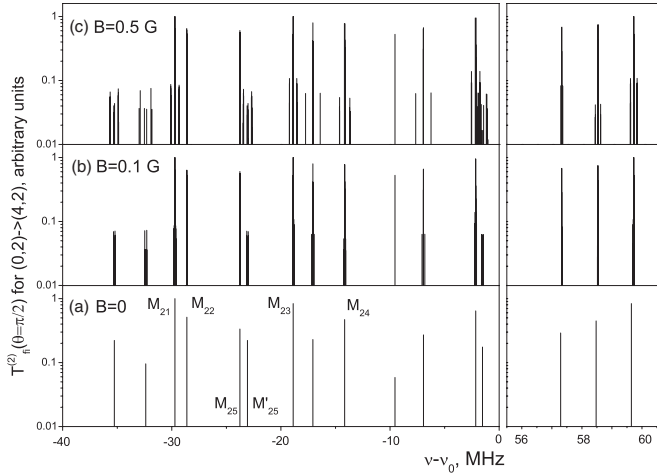


Figure 5. Strength $T_{fi}^{(2)}(\theta = \pi/2)$ of favoured hyperfine components of the $(\nu, L) = (0, 2) \rightarrow (4, 2)$ two-photon transition line, at $B = 0, 0.1$ and 0.5 G. The weighted mean frequencies for the Zeeman multiplets of the favoured hyperfine lines M_{21} – M_{24} are shifted at $B = 0.5$ G by up to 3 kHz.

field are shown in figure 5(a). In a transverse magnetic field ($\theta = \pi/2$) each of them splits into three components with $\Delta J_z = J'_z - J_z = -2, 0, 2$ with a typical separation of the order of $\sim 10^2$ kHz at $B = 0.5$ G; each of these components acquires an additional super-fine structure with separations in the $\sim 10^1$ kHz range (figures 5(b) and (c)). In a longitudinal magnetic field $\Delta J_z = 0$, and the lines undergo ‘super-fine’ splitting only. The weighted mean frequencies $\bar{\nu}_{\nu' L' n', \nu L n}(B)$ (see (12)) of the magnetic multiplets originating from the dominating hyperfine lines M_{21} – M_{24} in figure 5(a) are shifted by up to 3 kHz at $B = 0.5$ G, less than in one-photon transitions (cf table 4). Such a shift is tolerable for purposes of QED test/measurement of particle masses, but not for the purpose of searching for time dependence of fundamental constants.

The magnetic multiplets of closely lying pairs of hyperfine lines, such as M_{25} – M'_{25} on figure 5, may merge and need to be considered with account of the details of the line profile.

The optimal choice of the pair of the initial and final states for two-photon spectroscopy depends on several factors. In [8, 13] the importance of the presence of intermediate states with excitation energy close enough to $\nu_{fi}/2$ to enhance the transition rate has been discussed. A second factor is the population of the initial state, which may be enhanced by optical pumping [20]. Third, the strength of individual hyperfine lines is relevant; here transitions with a small number of components are favourable. Finally, the existence of magnetic components that are weakly sensitive to B guarantees that the systematic uncertainty is minimized.

Privileged candidates are the purely vibrational two-photon excitations of the ground state (see section 2.1), in particular the transition $(0, 0) \rightarrow (2, 0)$ whose hyperfine structure in zero field, in contrast to the general case discussed above, consists of only four distinct favoured lines (see figure 6) because the $L = 0$ states have only four levels (see figure 1) and the selection rules (ii) above imply no change of the quantum numbers for the favoured transitions.

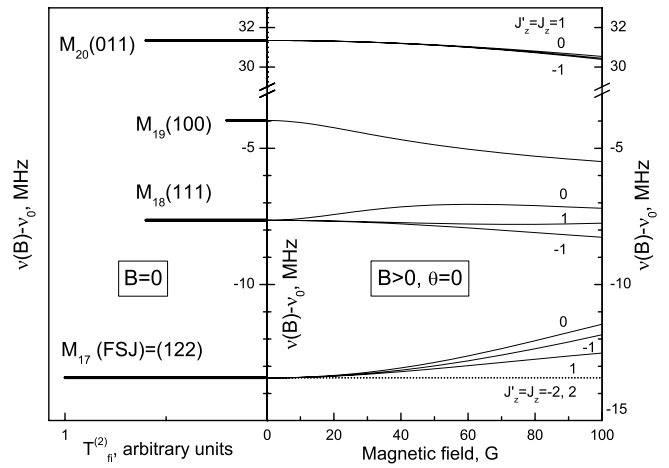


Figure 6. Left: strength $T_{fi}^{(2)}$ of the favoured components of the $(\nu, L) = (0, 0) \rightarrow (2, 0)$ two-photon transition line at $B = 0$, labelled with the quantum numbers $(FSJ) = (F' S' J')$. Right: Zeeman shift of the $\Delta J_z = 0$ components in the external magnetic field B . The spectrum is independent of θ . The transition frequencies between stretched states ($J_z = \pm 2$ components of M_{17} , dotted line) are independent of B .

The transition frequencies between levels with $L = 0$ in zero field can be given in simple analytical form. The only nonzero coefficients of the effective Hamiltonian $H_{\text{eff}}^{\text{hfs}}$ are E_4 and E_5 . In zero magnetic field, the four hyperfine levels have the following energy shifts, in order of increasing shift:

$$\begin{aligned} \Delta E^{v0(011)J_z} &= \frac{h}{4}(-E_4 - E_5 - \sqrt{4E_4^2 - 4E_4E_5 + 9E_5^2}) \\ \Delta E^{v0(100)J_z} &= \frac{h}{4}(E_4 - 4E_5) \\ \Delta E^{v0(111)J_z} &= \frac{h}{4}(-E_4 - E_5 + \sqrt{4E_4^2 - 4E_4E_5 + 9E_5^2}) \\ \Delta E^{v0(122)J_z} &= \frac{h}{4}(E_4 + 2E_5). \end{aligned} \quad (18)$$

The last of these is the state that also contains the stretched states with $J_z = \pm 2$.

At $B > 0$ each hyperfine level splits into $2J + 1$ magnetic subcomponents, leading to a total of 12 (favoured) subcomponents, which all have the same strength. The spectrum is identical for parallel and orthogonal polarization. This also means that the stretched-state transitions, which have zero shift and are degenerate, can be observed with arbitrary orientation of the magnetic field.

The Zeeman shift of the magnetic subcomponents is very weak: for 10 out of the 12 subcomponents the relative shift of the transition line is less than 2×10^{-12} at 1 G, and less than 2×10^{-13} at 0.3 G.

6. Discussion

A magnetic field splits the hyperfine components of the transition lines into sets of Zeeman subcomponents. The separation between the Zeeman subcomponents increases with B and reaches the order of magnitude of the hyperfine splitting

as B approaches the (state-dependent) threshold $B_{\text{thr}} \sim 5\text{--}50$ G. Above the threshold the transition spectra are rearranged.

The observable perturbing effects of a magnetic field depend on the spectroscopic resolution.

(1) *Low resolution (hyperfine structure unresolved)* The Zeeman shift of the weighted mean frequency defined by (12) for each favoured hyperfine components of a transition line is rather small (see table 4), e.g. less than 5×10^{-11} at 1 G for an overtone transition. If several such components combine into an unresolved line, the total shift is typically reduced even more.

(2) *Resolved hyperfine structure, unresolved Zeeman sub-levels* The level of spectroscopic resolution needed for improved measurements of mass ratios is about 10 kHz and therefore requires experimental resolution of the hyperfine structure, but not necessarily the ability to resolve the Zeeman sub-levels.

As we are interested in hyperfine lines that show weak magnetic shifts, resolving their individual Zeeman components at small bias fields $B < 1$ G may indeed be difficult. An example is the $L = 0 \rightarrow L' = 0$ two-photon transitions. The weighted mean of the Zeeman shifts of a multiplet should then be considered.

There exist two-photon transitions for which the systematic shift of the then unresolved multiplet will be small, e.g. -95 Hz at 1 G (-8×10^{-13}) for the $|vLFSJJ_z\rangle = |00(011)J_z\rangle \rightarrow |20(011)J'_z\rangle$ multiplet (the M_{20} line at 31.3 MHz in figure 6).

In the case of a one-photon transition, we mention the triplet of magnetic subcomponents $|01(010)J_z = 0\rangle \rightarrow |42(011)J'_z\rangle$ transition (see figure 3). The $J_z = 0 \rightarrow J'_z = 0$ subcomponent (parallel polarization) has the very small quadratic Zeeman coefficient of -7×10^{-14} G $^{-2}$ (shown in table 5), while the $J_z = 0 \rightarrow J'_z = \pm 1$ subcomponents (observable only in perpendicular polarization) have linear Zeeman shifts of 34.3 and -36.3 kHz at 1 G, respectively, with an averaged shift of only 290 Hz at 1 G (1.3×10^{-12}).

These shifts, where the worst case of non-optimal light polarization was assumed, are well below the current and near-future uncertainties of the theoretical transition energies and thus will not be a limitation in near-future comparisons of theoretical and experimental results.

(3) *Complete resolution* In this case many candidate transitions exist, both one-photon and two-photon transitions. Zero magnetic shifts are possible in the adopted approximation on $L = 0 \rightarrow L' = 0$ two-photon transitions involving stretched states. In the case of use of the symmetrically split one-photon or two-photon transitions between stretched states, it should be possible to measure each subcomponent independently and then compute the average which is free of shift. Such a procedure is standard in atomic optical clocks.

One technique applicable for cases 2 and 3 is quantum logic spectroscopy on a single HD $^+$ ion [21, 22], where the Lamb–Dicke confinement regime is attained and spectroscopic resolution at the level of the natural line width is possible. A second approach is conventional (absorption) spectroscopy of an ensemble of cooled, but not strongly confined molecular

ions of the two-photon or rotational spectroscopy type, which can also strongly suppress the Doppler broadening.

When spectroscopy of HD $^+$ is pursued with the goal of comparison with QED calculations and for a determination of the M_e/M_p , or M_e/M_d mass ratios, it may be important to determine the central frequency ν_0 of the vibrational transition. The theoretical value for ν_0 is now obtained with QED corrections up to the order $m\alpha^6$ and partially $m\alpha^7$ [15]. We propose to combine the results of two-photon spectroscopy between levels with $L = L' = 0$ with radiofrequency spectroscopy within the hyperfine structure of these levels to extract ν_0 . The coefficients of the effective spin Hamiltonian E_1, \dots, E_9 and, through (4), the spin-dependent corrections to E^{vL} can in principle be expressed in terms of the radiofrequencies of transitions within the hyperfine multiplet of the (vL) state (and similarly for the $(v'L')$ state). Since the number N_h of linearly independent hyperfine transition frequencies (3 for $L = 0$, 9 for $L = 1$ and 11 for $L \geq 2$) exceeds the number N_e of non-vanishing coefficients E_i , the above relations can be resolved for E_i either by obtaining the least-squares solution or by introducing $N_h - N_e$ additional compatibility relations the hyperfine frequencies that may serve to estimate the experimental accuracy. The value of ν_0 is therefore expressed uniquely in terms of spectroscopic data and may be used to test the predictions of few-body bound state QED in next-to-leading orders in α .

All these expressions become particularly simple for the rotationless $L = 0$ states, as was shown in section 5 (see (18)). Denoting the frequencies of the $J_z = 0 \rightarrow J'_z = 0$ components at $B = 0$ of three radiofrequency transitions in the $(v, L = 0)$ state by $\nu_1 = \nu_{v0(111)0, v0(100)0}$, $\nu_2 = \nu_{v0(122)0, v0(111)0}$, $\nu_3 = \nu_{v0(100)0, v0(011)0}$, and similarly, by ν'_1, \dots, ν'_3 , the corresponding frequencies in the $(v', 0)$ state, we have

$$E_4 = \nu_2 + \nu_3, \quad E_5 = 2(\nu_1 + \nu_2)/3,$$

with compatibility relation

$$\nu_2(\nu_1 + \nu_2 + \nu_3) = 2\nu_1\nu_3,$$

and similar for the v' state. The hyperfine energy of the $L = 0$ stretched states in zero field may be expressed as

$$\Delta E^{v0(122)\pm 2}/h = E_4/4 + E_5/2 = \nu_1/3 + 7\nu_2/12 + \nu_3/4.$$

The transition frequency between stretched states is $\nu_{v0(122)2, v'0(122)2} = \nu_0 + \Delta\nu$, $\Delta\nu = 1/3(\nu'_1 - \nu_1) + 7/12(\nu'_2 - \nu_2) + (\nu'_3 - \nu_3)/4$. Thus, ν_0 could be obtained by measuring one vibrational transition, and six radiofrequency transitions. The sensitivity to magnetic field comes only from $\Delta\nu$, since the Zeeman shift of $\nu_{v0(122)2, v'0(122)2}$ is strictly zero in the adopted approximation. For example, $\Delta\nu$ is shifted by only 55 Hz (5×10^{-13}) in the case $v = 0$, $v' = 2$ at $B = 1$ G. This shift value could be taken as a conservative estimate of the Zeeman uncertainty for ν_0 , but it could be further reduced by determining the magnetic field in the trap (essentially in real time) from a measurement of the Zeeman splitting of an appropriate microwave, one- or two-photon line and using the theoretical magnetic field sensitivities.

7. Conclusion

In conclusion, we have shown that both transitions weakly sensitive and insensitive to the magnetic field as well as symmetrically split doublets exist in the HD⁺ optical and THz (pure rotational) spectrum. In the spectroscopy of these transitions the Zeeman effect will not be a limiting factor for the experimental accuracy. This is of particular relevance to the possible use of HD⁺ transitions for setting limits to a hypothetical time dependence of particle mass ratios, where a relative inaccuracy at the level of 10⁻¹⁶ is desired.

We have also proposed how to experimentally obtain the central transition frequencies ν_0 between rotationless states of HD⁺ from a combination of frequency measurements of different radiofrequency transitions. By eliminating the contribution of the spin interactions, this approach allows us to suppress the contribution from particle magnetic moments and nuclear electromagnetic structure and to reduce theoretical and experimental uncertainties significantly. The QED energies and particle mass ratio determined by the comparison of experimental and theoretical results will therefore have a negligible contribution from magnetic field and nuclear structure effects.

The existence of transition pairs whose average frequency is independent of magnetic field is not affected by the higher order relativistic mass and anisotropy corrections to the electron-spin coupling term $E_{13}(\mathbf{S}_e \cdot \mathbf{B})$ since the latter only alter the Zeeman shift of the transition frequencies at the $O(\alpha^2) \sim 5 \cdot 10^{-5}$ level [7]. Thus, transitions with suppressed dependence on the magnetic field can be used as probes for high-order corrections to the magnetic Hamiltonian that would be enhanced by up to two orders of magnitude as compared to transitions with typical linear Zeeman shift.

Acknowledgments

The work was partly supported by grant 02-288 of the Bulgarian Science Fund (DB) and grant no 08-02-00341 of the Russian Foundation for Basic Research (VIK). DB and VIK also acknowledge the support from the Joint Institute for Nuclear Research within the collaboration program between

BLTP-JINR and INRNE-BAS. The work of SS has been performed in the framework of the DFG project Schi 431/11-1.

References

- [1] Fröhlich U, Roth B, Antonini P, Lömmerzahl C, Wicht A and Schiller S 2004 *Seminar on Astrophysics, Clocks and Fundamental Constants (Lecture Notes in Physics vol 648)* ed E Peik and S Karshenboim (Berlin: Springer) p 297
- [2] Schiller S and Korobov V I 2005 *Phys. Rev. A* **71** 032505
- [3] Koelemeij J C J, Roth B, Wicht A, Ernsting I and Schiller S 2007 *Phys. Rev. Lett.* **98** 173002
- [4] Kajita M 2008 *Phys. Rev. A* **77** 012511
- [5] Carrington A, McNab I R, Montgomerie-Leach C A and Kennedy R A 1991 *Mol. Phys.* **72** 735
- [6] Leach C A and Moss R E 1995 *Annu. Rev. Phys. Chem.* **46** 55
- [7] Hegstrom R A 1979 *Phys. Rev. A* **19** 17
- [8] Karr J-Ph, Kilic S and Hilico L 2005 *J. Phys. B: At. Mol. Opt. Phys.* **38** 853
- [9] Karr J-Ph, Korobov V I and Hilico L 2008 *Phys. Rev. A* **77** 062507
- [10] Karr J-Ph, Bielsa F, Douillet A, Pedregosa J, Korobov V I and Hilico L 2008 *Phys. Rev. A* **77** 063410
- [11] Bakalov D, Korobov V I and Schiller S 2005 *Proc. Int. Conf. on Exotic Atoms and Related Topics—'EXA 2005' (21–25 February, 2005)* (Austrian Academy of Sciences Press) p 401
- [12] Bakalov D, Korobov V I and Schiller S 2006 *Phys. Rev. Lett.* **97** 243001
- [13] Roth B, Koelemeij J, Schiller S, Hilico L, Karr J-Ph, Korobov V I and Bakalov D 2008 *Precision Physics of Simple Atomic Systems (Lecture Notes in Physics vol 745)* (Berlin: Springer) p 205
- [14] Korobov V I 2006 *Phys. Rev. A* **74** 052506
- [15] Korobov V I 2008 *Phys. Rev. A* **77** 022509
- [16] Korobov V I and Schiller S in preparation
- [17] Cohen-Tannoudji C, Diu B and Laloë F 1977 *Quantum Mechanics vol 1* (New York: Wiley) p 831
- [18] Colbourn E A and Bunker P R 1976 *J. Mol. Spectrosc.* **63** 155
- [19] Cagnac B, Grynberg G and Biraben F 1973 *J. Phys. (Paris)* **34** 845
- [20] Schneider T, Roth B, Duncker H, Ernsting I and Schiller S 2010 *Nature Phys.* **6** 275
- [21] Rosenband T *et al* 2007 *Phys. Rev. Lett.* **98** 220801
Schmidt P O *et al* 2005 *Science* **309** 749
- [22] Bergquist J C, Wineland D J and Itano W M 1985 *Phys. Rev. Lett.* **55** 1567